Norwegian Meteorological Institute
met.no

met.no report

no. 11/2007
Remote sensing

First results from comparison of model calculated AOD with MODIS data

AeroKval project report

Svetlana Tsyro, Hanne Heiberg,
Heiko Klein, Harald Schyberg, Leonor Tarrasón,
and Jan Eiof Jonson

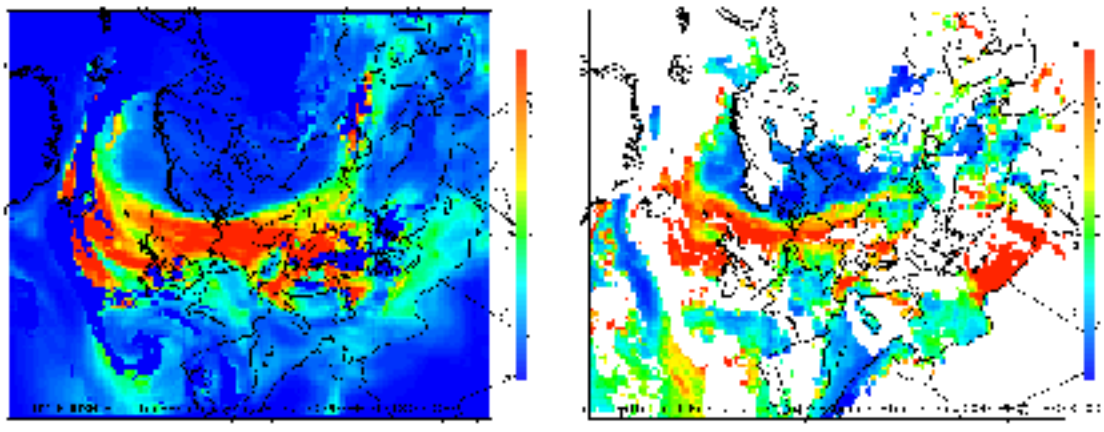

AOD at 0.55 μm on 1 April 2004, as calculated by the EMEP model (left) and measured by MODIS (right)

Norwegian Meteorological Institute
met.no

report

Title	Date
First results from comparison of model calculated AOD with MODIS data	10 December 2007
Section	**Report no.**
Air Pollution and Remote Sensing, R&D Department.	11
Author(s)	**Classification**
Svetlana Tsyro, Hanne Heiberg, Heiko Klein, Harald Schyberg, Leonor Tarrasón, and Jan Eiof Jonson	☒ Free ☐ Restricted
	ISSN 1503-8025
	e-ISSN
Client(s)	**Client's reference**
Norwegian Space Centre	

Abstract

Satellite observations of aerosol optical depth (AOD) provide information about the variation and location of aerosols, and can be used in monitoring and forecasting air quality. As a first step towards an operational system for aerosol forecasting, an observation operator for AOD has been developed and implemented in the EMEP chemical transport model. First results for AOD at 0.55μm simulated by the EMEP model have been compared with AOD observations from the MODIS instruments. On average, the model underestimates MODIS AOD by about 50% for warm seasons and by about 20% for cold seasons. The spatial correlation is below 0.35 for the whole EMEP grid, while the temporal correlation mostly lies between 0.4 and 0.6 for different regions and EMEP sites. The differences between the simulated and observed AOD, as well as the uncertainties in model and MODIS AOD have been discussed.

Keywords

Satellite aerosol observations, MODIS aerosol products, AOD, chemical transport model.

Disiplinary signature	Responsible signature

Postal address: P.O.Box 43, Blindern, NO-0313 OSLO, Norway
Office: Niels Henrik Abelsvei 40
Telephone: +47 22 96 30 00
Telefax: +47 22 96 30 50
e-mail: met@met.no
Internet: met.no
Bank account: 7694 05 00628
Swift code: DNBANOBK

Postal address
P.O.Box 43, Blindern
NO-0313 OSLO
Norway

Office
Niels Henrik Abelsvei 40

Telephone
+47 22 96 30 00

Telefax
+47 22 96 30 50

e-mail: met@met.no
Internet: met.no

Bank account
7694 05 00628

Swift code
DNBANOBK

1. Introduction

Satellite data from the MODIS instruments provide information about aerosols and chemical components that influence the air quality. Such observations can be exploited in monitoring and forecasting air quality together with chemical transport models, which describe advection, diffusion and chemical transformations of trace gases and aerosols in the atmosphere. Although this does not reduce the air pollution by itself, it facilitates increased control of the problem, and gives the authorities the chance to take immediate actions to reduce hazards. A significant part of aerosol pollution is due to anthropogenic emissions. There are strong evidences that atmospheric aerosols have adverse effects on human health. According to recent model estimates, current exposure to PM (Particulate Matter, i.e. aerosols) from anthropogenic sources leads to loss of 8.6 months of life expectancy in Europe. Around 348 000 of premature deaths and some 100 000 hospital admissions can be attributed to PM exposure annually in the EU (25 countries) (WHO, 2006).

Making use of satellite observations is a relatively recent practise in assessing the chemical state of atmosphere. Until the last decade, ground-based measurements of pollutant surface concentrations were mostly employed for monitoring air pollution and for model validations. Compared to ground-based measurements (surface measurements and remote sensing), air pollution monitoring from the satellites has several advantages. Covering practically the whole globe, satellite observations represent valuable data for models evaluation, facilitating validations of model results for very different chemical and meteorological regimes, particularly in the regions with a lack of surface monitoring. Furthermore, LIDARs onboard satellites provide important information about pollutant vertical profiles. Finally, satellite measurements, available in the near-real time regime, can be assimilated within model forecasts of the chemical weather in order to improve the prediction accuracy.

For optimal use of satellite data in monitoring and forecasting, all relevant satellite observations should be integrated with information from a chemical transport model. The general approaches of data assimilation, which were developed e.g. for numerical weather prediction, can be adapted and further developed for improved monitoring and forecasting of aerosol air pollution.

As a first step towards an operational system for aerosol forecasting the AeroKval project has focused on three work packages:

1. Develop and implement an observation operator to the EMEP chemical transport model, which simulates aerosol observations from the MODIS instruments aboard the Aqua and Terra satellites.
2. Compare model simulation results with MODIS aerosol observations and analyse the results.
3. Outline a strategy for optimal use of satellite observations for forecasting and monitoring of air quality.

This report describes the results of work package 1 and 2, while the results of work package 3 are described in a separate report.

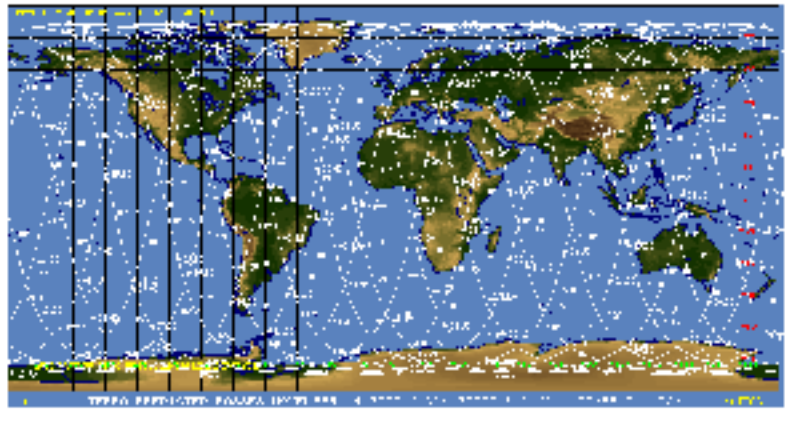

Figure 1: *Example Terra orbit ground tracks for a single day.*

2. MODIS data

2.1 General characteristics

The Moderate resolution Imaging Spectrometer (MODIS) onboard the NASA polar-orbiting earth observation satellites Aqua and Terra detects radiances in the visible and infrared spectrum region over all oceans and most of the continents at least once daily (Fig. 1). The MODIS aerosol products provided by NASA include primary retrieved parameters (e.g. aerosol optical depth (AOD), Fine mode Weighting and effective radius) and derived parameters (e.g. asymmetry factor, backscattering ratio and Ångström exponent). Daily Level 2 multi-parameter data are produced in 5 min. orbital swath slices (granules) with spatial resolution of 10 km * 10 km (at nadir). Each granule is about 2030 km along the orbital path and has a swath about 2330 km, consisting of 135 * 203 boxes of retrieved Level 2 data, see Fig. 2. Each box of retrieved data is based on 10 * 10 = 100 "1 km" pixels and 20 * 20 = 400 "500 m" pixels. These resolutions refer to nadir view. Due to spherical geometry, the size of each "1 km" pixel increases from 1 km at nadir to nearly 2 km at the swath edges.

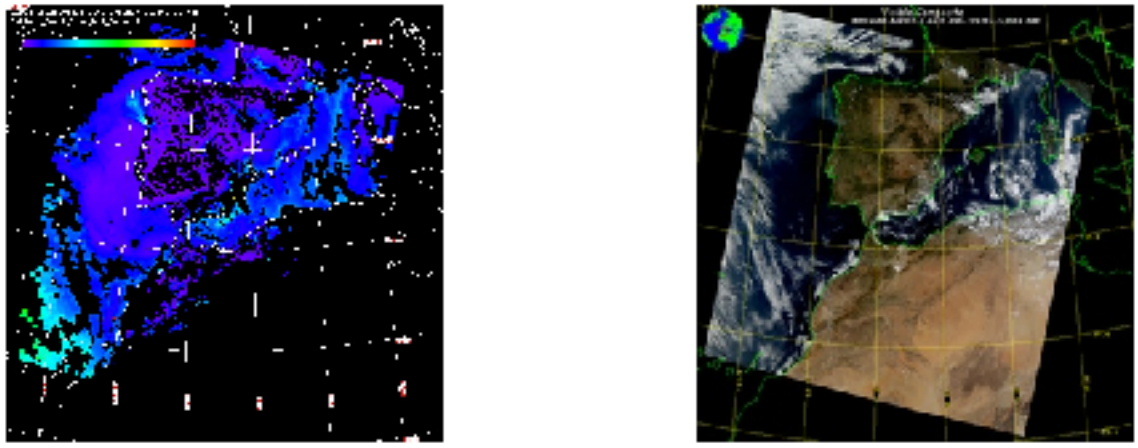

Figure 2: *Examples of MODIS images for Spain, north Africa and surrounding N. Atlantic.* ***Left:*** *Aerosol optical depth (AOD) observations. The colour scale goes from 0.0 (purple) to 1.0 (red).* ***Right:*** *MODIS RGB image, i.e. representation of measurements from three MODIS channels in a weighted combination of red, green and blue.*

2.2 Aerosol retrievals

The aerosol retrieval algorithm uses data in the visible spectrum region, so only daytime data are considered for retrieval. The present study is based on the data from "Collection 5" which are data reprocessed with the most recent retrieval algorithms. A short description of the retrieval algorithm follows. For further details, see the algorithm description by Remer et al. (2006). The MODIS algorithm uses the reflectance (ρ_λ), defined as a function of the measured spectral radiance (L_λ), the solar zenith angle (θ_0), and the solar irradiance F_0 in the wavelength band λ

$$\rho_\lambda = L_{ext} \frac{\pi}{F_{0,\lambda} \cos(\theta)} \qquad (1)$$

The reflectance in all MODIS-aerosol channels is corrected for extinction by the water vapour, ozone, and carbon dioxide based on climatology data. Observations over land and ocean are processed with two separate algorithms, so each pixel is identified as either land or ocean. If all pixels in the 10x10 km^2 box are considered water, the processing proceeds with the **over-ocean** retrieval algorithm. Next, cloud, sun glint and sediment masks are applied, and the contaminated pixels are identified and discarded. As clouds normally show higher variability in reflectance than aerosols, the cloud mask combines spatial variability

tests along with tests of brightness in visible and infrared channels. Underwater sediments can contaminate measurements over shallow waters, e.g. near coastlines. The sediment mask takes advantage of the strong absorption by water at wavelengths longer than 1 μm. The resulting spectral reflectances over water with suspended sediments thus show elevated values in the visible, but not in longer wavelengths. This creates a unique spectral signature quite different from clear ocean water and also different for airborne dust. The ocean algorithm is designed to retrieve only over dark ocean, i.e. away from sun glint regions. Therefore, a sun glint mask is used in order to avoid glint contamination of retrieved data. Before discarding, the glint pixels are checked on the presence of heavy dust over glint. The over-ocean retrieval makes use of seven wavelength bands and a number of extra bands to help with cloud and other screening procedures.

If at least 2.5% of (non-masked) pixels remain in the box, the algorithm proceeds to calculate the aerosol optical depth in an inversion procedure. The inversion part of the algorithm is based on a look-up table approach with pre-computed spectral reflectances for a set of aerosol and surface parameters. The climatology used for the look-up table is mainly based on measurements by sun/sky photometers (AERONET; Holben et al., 1998). The algorithm provides four fine aerosol modes and five coarse modes. It is assumed that a properly weighted combination of one fine and one coarse log-normal aerosol mode (called "aerosol model") can represent the ambient optical and physical aerosol properties over the target. Spectral reflectances of the possible combinations of modes are compared with the MODIS measured spectral reflectance to find the "best" (least-square) fit. The fit, or an "average" of several "best" fits, is the solution to the inversion.

The **over-land** retrieval algorithm discards pixels with clouds, in-land water bodies and snow/ice. Like the ocean algorithm, the land algorithm does inversion using a look-up table. It is assumed that one fine-dominated aerosol model and one coarse-dominated aerosols model (where each may be comprised of multiple lognormal modes) can be combined with proper weightings to represent the ambient aerosol properties. The land retrieval algorithm uses a priori assigned fine aerosol types ("aerosol models"), depending on the geographical location and the season. Three types of fine aerosol models are defined: non-absorbing (urban/industrial), absorbing (savanna/grass smoke) and neutral (forest smoke), which are assumed to be spherical. In addition, one type of spheroid aerosol represents coarse dust particles. Observations of spectral reflectance in three channels are used for over-land retrieval of AOD.

2.3 MODIS data used in this work

The data are provided by the Goddard Space Flight Center (NASA), and has been downloaded from their data archive by the interactive web portal http://ladsweb.nascom.nasa.gov/index.html. MODIS AOD from the Terra platform is available from 2001 and from the Aqua platform from 2003. We have chosen a subset of data representing different seasons of the year: July-August, November-December in 2003, and March-April, and July-August in 2004.

The archived aerosol products are stored in multi-parameter Hierarchical Data Format (HDF), as one granule per file. Each granule consists of 203 (204) 10-km boxes along the satellite track, times 135 10-km boxes perpendicular to the satellite track. For his work, two dimensional aerosol products have been extracted from the downloaded HDF files, and their hourly and daily averages have been aggregated in the EMEP grid with 50 x 50 km^2 resolution (see map in Fig. 4). The aggregated MODIS aerosol data are stored in NetCDF format, which facilitates comparison with results from the EMEP chemical transport model.

2.4 Uncertainties and limitations of MODIS data

In the present work, we have used the MODIS product called "Optical_Depth_Land_And_Ocean", which contains data for AOD at 0.55 μm. This MODIS data set was chosen for the present work because it

- relies on primary retrieved data only;
- has most stringent quality control;
- is a joint product, covering both land and ocean.

The expected error-bars of AOD are $\Delta\tau = \pm 0.03 \pm 0.05\tau$ over ocean and $\Delta\tau = \pm 0.05 \pm 0.15\tau$ over land. While in general the MODIS retrievals meet the expected accuracy, under certain conditions they do not. The main data uncertainties over ocean are due to the effect of non-spherical dust and cloud contamination, particularly low altitude ice clouds at high latitudes. The main uncertainties over land are due to cloud contamination, and surfaces with sub-pixel snow, ice or surface water (coastal regions, marshes, etc.). Furthermore, pre-assigned aerosol optical models for over-land retrieval lead to either positive or negative bias for large AOD in many regions. Choosing optimal refractive indices for the different chemical components is not a straightforward task, and is another source of uncertainties.

The MODIS algorithm checks and discards pixels in order to avoid different types of contamination as described above. The algorithm requires that minimum 2.5% of the pixels remain to produce an AOD value for a 10x10 km^2 box. Further the MODIS AOD product values are aggregated to give an AOD for each of the 50x50 km^2 EMEP grid cells. The representativeness of MODIS AOD may therefore vary considerably from grid cell to grid cell.

3. Implementation of AOD calculations in the EMEP model

3.1 Short description of the EMEP model

The EMEP aerosol model is a 3-D Eulerian model, which calculation domain covers the whole Europe. The model uses a polar-stereographic projection, true at 60°N, and has a horizontal resolution of 50x50 km^2. A normalized pressure coordinate (σ-coordinate) is used to define the model vertically, with 20 layers resolving the vertical calculation domain (up to ca. 100 hPa).

The model describes the emissions, chemical transformation, transport, dry and wet deposition of atmospheric aerosols and their gaseous precursors, as well as the aerosol dynamics processes. The aerosol model currently uses the simplified photo-chemical scheme of the EMEP Unified model and includes 14 chemical prognostic components: 7 gases - SO_2, H_2SO_4, NO, NO_2, HNO_3, PAN, NH_3; and 7 aerosol components – sulphate (SO_4^{2-}), nitrate (NO_3^-) ammonium (NH_4^+), anthropogenic primary organic carbon (APOC), elemental carbon (EC), mineral dust, and sea salt (Table 1). The aerosol water content is calculated based on the chemical composition of aerosols and ambient relative humidity.

Table 1: *Size-dependent aerosol parameters calculated with the EMEP aerosol model*

	N	SO_4^{2-}	NO_3^-	NH_4^+	EC	APOC	Dust	Sea salt	water
Nucleation D< 0.02 μm	X	X							X
Aitken 0.02 <D< 0.1 μm	X	X	X	X	X	X		X	X
Accumulation 0.1 <D< 2.5 μm	X	X	X	X	X	X	X	X	X
Coarse 2.5 <D< 10 μm	X	X	X		X		X	X	X

Here, N is the particle total number concentration, and the others are the mass concentrations of aerosol components

The model describes the aerosol size distribution with four size fractions (modes): nucleation (particles with diameters d < 0.02μm), Aitken (0.02μm < d< 0.1μm), accumulation (0.1μm < d < 2.5μm), and coarse (2.5μm d < 10.0μm) (Table 1). The underlying assumption is that the aerosols are internally mixed and monodisperse within each of the four size fractions (i.e. all particles within the same fraction have the same chemical composition and the same size (Pirjola et al., 2003). The aerosol relevant processes are calculated in the EMEP aerosol mode with the aerosol dynamics module MONO32, which accounts for particle

nucleation, condensation and coagulation processes (Pirjola et al., 2002). The aerosol model calculates particle number and mass concentrations for each aerosol component distributed for the four size modes and concentrations of PM_{10} and $PM_{2.5}$ (i.e. Particulate Matter, or particles with diameters smaller than 10 and 2.5 μm respectively).

Input data to the aerosol model includes emissions of gaseous aerosol precursors, i.e. sulphur oxides (SO_x), nitrogen oxides (NO_x) and ammonia (NH_3), as well as primary PM_{10} and $PM_{2.5}$ emissions. The emission data are from the EMEP emission database. All emissions are distributed horizontally over the EMEP grid and high emissions are distributed between the vertical layers. Further, the emissions are disaggregated by month and day-of-week, using the scaling factors obtained from the GENEMIS project (Generation and Evaluation of Emission Data Project, **http://genemis.ier.uni-stuttgart.de/),** and between day and night. The chemical speciation of PM emissions is made using the inventory of OC and EC emissions in Europe developed by Kupiainen and Klimont (2006). The PM emissions are allocated between organic carbon (OC), elemental carbon (EC) and inorganic PM (mineral dust).

Presently, there is no appropriate information available with respect to size distribution of PM emissions. Therefore rather crude assumptions are made in the EMEP aerosol model to calculate the size distribution of particle emissions from PM mass emissions. The emissions of fine OC and EC are distributed between the Aitken and the accumulation fractions. Finally, PM number emissions in the Aitken, accumulation and coarse fractions are derived from the PM mass emissions, using assumptions on the particle mean diameters for each size fraction and the densities of PM components (Tsyro, 2003).

Production of sea salt aerosols from sea spray is calculated based on parameterisations of Monahan et al. (1986) and Mårtensson et al. (2003). The parameterisation of windblown dust is developed based on works of Marticorena and Bergametti (1996), Gomes et al. (2003) and references therein. The comprehensive description of the EMEP aerosol model is given in Simpson et al. (2003), Tsyro (2004).

3.2 Aerosol Optical Depth calculation

3.2.1 Basics

Aerosol optical depth (AOD) describes the extinction of light beam traversing an atmospheric layer containing aerosol particles. Light extinction by aerosols occurs by attenuation of the incident light due to scattering and absorption. AOD within the atmospheric layer between z_1 and z_2 (τ_{ext}) is calculated as

$$\tau_{ext} = \int_{z1}^{z2} k_{ext}(\lambda, r)dz \qquad (2)$$

Here k_{ext} is the aerosol extinction coefficient at height z. z_1 and z_2 are the heights of the layer bottom and top.

$$k_{ext}(\lambda,r) = \int_{r1}^{r2} C_{ext}(\lambda,r) \cdot N dr = \int_{r1}^{r2} \pi \cdot r^2 \cdot Q_{ext}(\lambda,r) \cdot N dr \qquad (3)$$

where r is the aerosol radius, N is the aerosol number density, r_1 and r_2 are the lower and upper radii of the particle size distribution, C_{ext} is the aerosol extinction cross-section, Q_{ext} is the aerosol extinction efficiency, so that $C_{ext}(\lambda,r) = \pi \cdot r^2 \cdot Q_{ext}$. Both C_{ext} and Q_{ext} are functions of the particle size and the light wavelength (λ).

The absorption and scattering of light by spherical particles is described by Mie theory. The key parameters that govern the scattering and absorption of light by a particle are (1) the wavelength of the incident radiation, (2) the size of the particle, which are combined in a dimensionless size parameter $\alpha = 2\pi r/\lambda$, and (3) the complex refractive index of the particle relative to the surrounding air: $m = n+ik$, where n and k denote the non-absorbing (scattering) and absorbing parts. Complex refractive index is a specific material's property, and it is believed to apply down to the material's smallest particle. Based on the value of particle

size parameter, three main domains of light scattering can be identified: Rayleigh scattering ($\alpha << 1$), Mie scattering ($\alpha \cong 1$), and geometrical scattering ($\alpha >> 1$).

3.2.2 AOD observation operator

We have developed a FORTRAN module, which we call "observation operator", for simulations of AOD. This AOD module can either be used online within the EMEP aerosol model (as it is done currently) or be used independently based on the aerosol concentration results from the transport model. In present work, the observational operator has been used to calculate AOD at only one wavelength of 0.55 μm. However, it can be used for calculating AOD at any wavelength.

The scheme is based on the Mie scattering mathematical formalism. The particles are assumed to be spherical and internally mixed. Two AOD schemes have been tested within the model: a simplified one based on aerosol mass concentrations and the one using particle number size distribution and Mie theory.

AOD based on aerosol mass. The formula for AOD is derived from equation (2) and (3) as

$$\tau = \int_{z1}^{z2} \pi \cdot r^2 \cdot Q_{ext} \cdot N dz = \int_{z1}^{z2} \int_{r1}^{r2} \frac{4}{3} \pi \cdot r^3 \cdot N \cdot \rho) \cdot Q_{ext} \frac{3}{4r\rho} dr\, dz = \int_{z1}^{z2} \int_{r1}^{r2} m \cdot E_{ext} dr dz \qquad (4)$$

where m [g/m^3] is the aerosol mass concentration and E_{ext} [m^2/g] is the mass specific cross-section. This is implemented in the model as

$$\tau = \sum_{k=1}^{ktop} \sum_{i=1}^{i=8} (m_i \cdot E_{ext,i}) \Delta z_k \qquad (5)$$

where m_i is the concentration, $E_{ext,i}$ is the mass specific cross-section for the aerosol component i (i =1, 8), Δz is the depth of model vertical layer, and k=*1* and k=*ktop* are the bottom and the top layers in the model. The values of mass specific extinction cross-section for aerosol components used in the EMEP model are provided in Table 2.

Table 2: *Mass specific cross-sections (m^2/g).* (Tegen et al., 1997; Seinfeld & Pandis, 1997; Kinne et al., 2005)

	SO_4	NO_3	NH_4	OC	EC	Min. dust	Sea salt
E_{ext} wet	8.5	8.5	8.5	5.0	9	0.9	0.4
E_{ext} dry	5.0	5.0	5.0	5.0	9.0	0.9	0.2
GF*)	1.7	1.7	1.7	1.3	1.0	1.0	2.0

*) GF denotes the Growth Factor of aerosol particles due to adsorption of water by soluble components, and is a ratio between the radius of dry particle and the radius of the particle with associated water at ambient relative humidity.
"E_{ext}wet" represents mass specific cross-sections for wet aerosols, i.e. implicitly accounts for aerosol water. "E_{ext}dry" are the mass specific cross-sections for dry aerosols; in the model, they are multiplied by GF to accounf for aerosol water

AOD based on particle number size distribution. The formula for AOD calculation based on the particle size number distribution is written as

$$\tau = \int_{z1}^{z2} \int_{r1}^{r2} \pi \cdot r^2 \cdot Q_{ext}(\lambda, r) \cdot N dr\, dz \qquad (6)$$

The extinction efficiency is calculated using the Mie scattering formalism and based on an effective complex refractive index for each of the four size fractions. As a first approximation, the effective complex

refractive index is calculated as the sum of volume weighted complex refractive indices of all aerosol components, including aerosol water, as

$$m_{eff} = \Sigma (v_i \cdot n_i) + i \, \Sigma(v_i \cdot k_i) \qquad (7)$$

where v_i is the volume fraction of a component i to the total volume in the size bin (i = 1,8).

It should be pointed out that the effect of aerosol water is explicitly accounted for in this approach. The scattering is a complex function of both refractive index and particle size. Increase in ambient relative humidity leads to a larger water uptake by aerosols, which causes aerosol growth, while both the real and imaginary parts of their refractive index tend to decrease. In fact, decrease in refractive index as relative humidity increases is not large enough to counteract the increase of the particles' cross-section due to size increase. Thus, aerosol water uptake with increase in relative humidity will lead to an increase in aerosol scattering.

This approach gives a reasonable estimate for effective refractive index in many cases. However, some research results indicate that the plain volume mixing approach may slightly exaggerate the absorption under certain circumstances and suggest using the Maxwell Garnett Mixing rule

$$m_{eff}^{\ 2} = m_0^{\ 2} \frac{m_{EC}^{\ 2} + 2m_0^{\ 2} + 2v_{EC}(m_{EC}^{\ 2} - m_0^{\ 2})}{m_{EC}^{\ 2} + 2m_0^{\ 2} - v_{EC}(m_{EC}^{\ 2} - m_0^{\ 2})} \qquad (8)$$

(Chýlec et al., 1998; Kirkevåg et al., 2005) for elemental carbon, which totally dominates the absorption (k in Table 3). m_{EC} is the refractive index of elemental carbon and m_0 is the sum of volume weighted refractive indices of the other (approximately non-absorbing) aerosol components as given in equation (7). We envisage implementing and testing the Maxwell Garnett Mixing rule on a later stage. The real and imaginary parts of complex refractive index for aerosol components adopted in the present work are provided in Table 3.

***Table 3**: Real (n) and imaginary (k) parts of the complex refractive index (m = n + ik) for different aerosol components adopted in the EMEP model calculations*

	SO_4^{2-} [1]	NO_3^- [1]	NH_4^+ [1]	OC [1]	EC [2]	Min. dust [3]	Sea salt [2]	Water [4]
n	1.43	1.43	1.43	1.53	1.95	1.5	1.56	1.333
k	10^{-8}	10^{-8}	10^{-8}	0.006	0.79	10^{-8}	0.0025	0.0

The sources are: [1] Köpke et al. (2006), [2] Bond and Bergstrom (2006), [3] Sokolik and Toon (1999), [4] Hale and Querry (1973)

We made use of a code for Mie scattering calculations, developed by Mishchenko and freely available on Internet (Mishchenko, 2005). Running Mie calculations online with the aerosol transport model is very CPU demanding. We have therefore made a lookup table for extinction efficiency (Q_{ext}) and extinction cross-section (C_{ext}) at 0.55 μm. The table allows finding Q_{ext} for a given particle radius and a complex refractive index (m_{eff}). To optimise the size of the lookup table, we first calculated the possible ranges for real (n) and imaginary (k) components of the refractive index for λ=0.55 μm, changing the relative contributions of components in the particle, which covered all possible particle chemical compositions.

Thus, the lookup table made is a 3-dimensional table, with r, n and k being the input parameters, varying within the following ranges: 0.5nm < r < 20μm, 0.0 < k < 1.0, while the range of n values changes for different k, so that 1.1 < n < 2.5 (the calculated ranges of n shown in Fig. 1, are extended in the lookup table to assure computational robustness). The following increments for these input parameters have presently been used: the ranges of n and k values were divided respectively onto 18 and 20 equal intervals, and the range of r values was divided onto 23 intervals of a variable size.

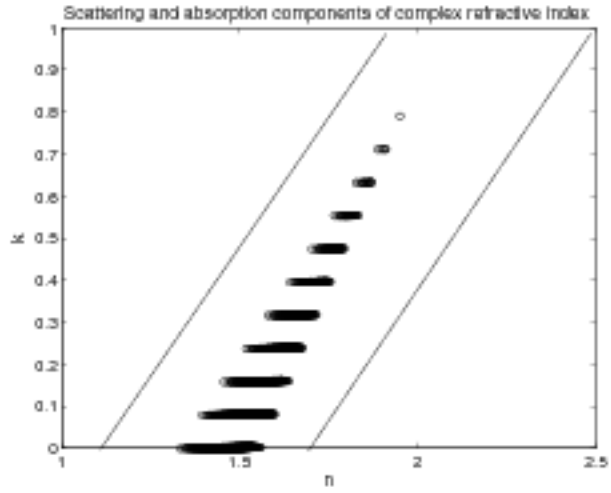

Figure 3: *Calculated scattering (n) and absorbing (k) parts of the effective refractive index, m = n +ik, for λ=0.55 μm, by changing the volume contribution of each component (namely, SO_4^{2-}, NO_3^-, NH_4^+, OC, EC, mineral dust, sea salt and water) from 0% to 100% with a step of 10%. This covers in principle all possible particle chemical compositions.*

Mishchenko's Mie scattering program allows calculating the aerosol light extinction properties for several different particle size distributions. Two lookup tables were made: one table for monodisperse distribution and one table for log-normal particle distribution within each of four size fractions in the aerosol model. When calculating Mie-scattering for log-normally distributed aerosols, we used the same standard deviations as those assumed in the EMEP model. The resulting extinction efficiencies at 0.55 μm for log-normal aerosol distribution within the size fractions are somewhat larger than those for monodisperse aerosols.

Implementation of AOD scheme in the EMEP model.

The AOD formula is implemented in the EMEP model in a discretised form as

$$\tau = \sum_{k=1}^{ktop} (\pi r_i^2 N_i \cdot Q_{ext,i}) \Delta z_k \qquad (9)$$

where N_i, r_i, and $Q_{ext,\,i}$ are the number density, the radius, and the extinction efficiency for particles in size fraction *i*.

AOD is calculated at every advection time step (20 min) based on model calculated concentrations of aerosol components and particle number densities for the four size modes in all model vertical layers. The lookup table for aerosol extinction efficiency was used as an input in the EMEP model. At each advection time step, new effective real and imaginary parts of complex refractive index, i.e. *n* and *k*, are calculated. Together with calculated particle radius, *n* and *k* are used to find extinction efficiency from the lookup table by a linear interpolation of tabulated Q_{ext} with respect to *r*, *n* and *k*.

4. Preliminary model AOD results and comparison with MODIS data

4.1 AOD distribution over Europe

The EMEP aerosol model has been used to calculate AOD at 0.55 μm wavelength for the years 2003 and 2004. Three different approaches (schemes) to calculate AOD have been tested and presented in this report. These are: 1) AOD based on aerosol mass concentrations and using the mass specific scattering cross-sections (hereforth, mass-based AOD), 2) AOD based on aerosol size number distribution using Mie scattering lookup table for monodisperse aerosols (hereforth, Mie-mono AOD), and 3) AOD based on aerosol size number distribution using Mie scattering lookup table for log-normally distributed aerosols (hereforth, Mie-lognor AOD) within the size fractions. Examples of first model results for aerosol optical depth are given in Figure 1, which shows annual mean calculated maps of AOD at 0.55 μm wavelength over Europe for 2004. AOD shown in Fig. 1(a) has been calculated using the aerosol mass-based scheme, while AOD in Fig. 1(b) and 1(c) has been calculated based on aerosol number size distribution, using Mie scattering formulation for monodisperse and log-normally distributed particles respectively.

The distribution of mass-based AOD appears to be considerably affected by Saharan dust, which is a result of calculated large concentrations of light-scattering dust. On the other hand, in the distribution of Mie-based AOD, the contributions to AOD from secondary inorganic aerosols, SO_4^{2-} (with max due to Etna emissions), NO_3^- and NH_4^+ (typical max in Benelux), and sea salt aerosols over sea are pronounced in the geographical AOD distribution. It is seen that calculations based on Mie-lognor approach yield the largest AOD values than Mie-mono AOD all over, and larger than mass-based AOD over Europe.

Some of likely reasons for the discrepancies between modelled mass-based AOD and Mie-based AOD are:

1. Different model ability with respect to reproducing aerosol mass concentrations and aerosol number concentration and size distribution. The model calculates aerosol mass concentrations more accurate than aerosol number size distribution due to the lack of data on particle emission size distribution and uncertainties in modelling aerosol dynamics processes;
2. Different approaches for calculating aerosol scattering properties. Namely, mass specific scattering cross-section, same for both fine and coarse aerosols, have been used for mass-based AOD, while complex refractive indices have been used to calculate aerosol scattering efficiencies for four size fraction in Mie-based AOD. The latter approach is believed to be more physically sound and adequate.
3. Different treatment of aerosol water. For mass-based AOD, aerosol water has implicitly (rather crudely) been accounted in mass specific scattering cross-sections of soluble components, while in Mie-based AOD scheme, extinction by aerosol water is explicitly calculated for each size fraction.

Figure 5 shows the seasonal variation of model calculated AOD in 2004. Calculated AOD is larger in a winter-early spring period (e.g. March and December) compared to summer (July) over most of Europe. This is due to larger anthropogenic emissions (in particular, from residential and commercial combustion sources) and because of more stable atmospheric conditions inhibiting pollutant dispersion and less efficient dry deposition.

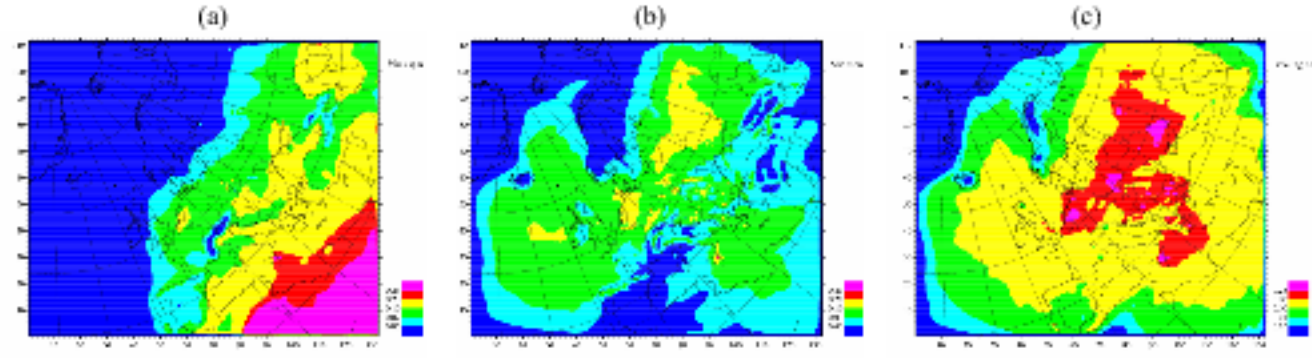

***Figure 4**: Annual mean calculated AOD for 2004: **(a)** based on the simplified scheme using aerosol mass concentrations (mass-basedAOD) and based on Mie scattering for **(b)** monodisperse(Mie-mono) and **(c)** log-normally distributed (Mie-lognor) aerosol.*

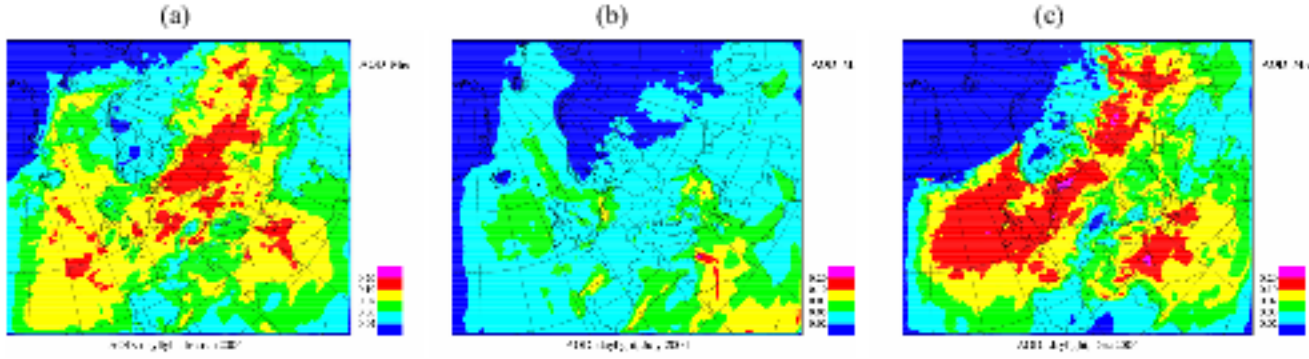

***Figure 5:** Seasonal variation of calculated AOD in 2004. Monthly mean Mie-lognor AOD for: **(a)** March, **(b)** July, and **(c)** December*

4.2 Comparison with MODIS data

Model calculated AOD has been compared with MODIS AOD retrievals for several periods representing different seasons, namely, July-August and November-December in 2003 and March-April and July-August in 2004 (see Section 2). Daily mean AOD values from the model and MODIS data have been compared for grid cells of the EMEP grid. To provide a more consistent comparison, calculated AOD have been averaged for hours with the sunlight and with cloud cover less than 50% in the model.

Fig.6 shows some examples of daily mean modelled and MODIS AOD, for arbitrary days: 1 August and 1 December 2003, and 1 April 2004. A very good match between calculated Mie-lognor AOD (Fig.6c, middle panels) and MODIS AOD (Fig.6c, lower panels) is obtained for 1 April 2004. For this day, the model captures very well the pattern of enhanced AOD, over the North Atlantic and the North Sea due to sea salt spray, stretching across Germany and Czech republic eastwards, in the Po Valley. Also for 1 August 2003, the model reproduces quite well the pattern of MODIS retrieved AOD over most of Europe (Fig.6a). For instance, it captures the enhanced AOD over Benelux and Denmark, over Hungary, Austria and Bulgaria, in the N. Atlantic west to Ireland and the Mediterranean Sea. On the other hand, the model does not reproduce rather high AOD due to Saharan dust intrusion in the south of Spain, which was detected by MODIS. The maps for 1 December illustrate the situation with much worse data coverage of MODIS AOD data. AOD retrievals were missing for almost entire Europe, probably due to the presence of clouds, snow/ice coverage (short or absent light day) in higher latitudes. Also, calculated mass-based AOD are shown for 1 August and 1 April 2004 (Fig. 6, upper panels).

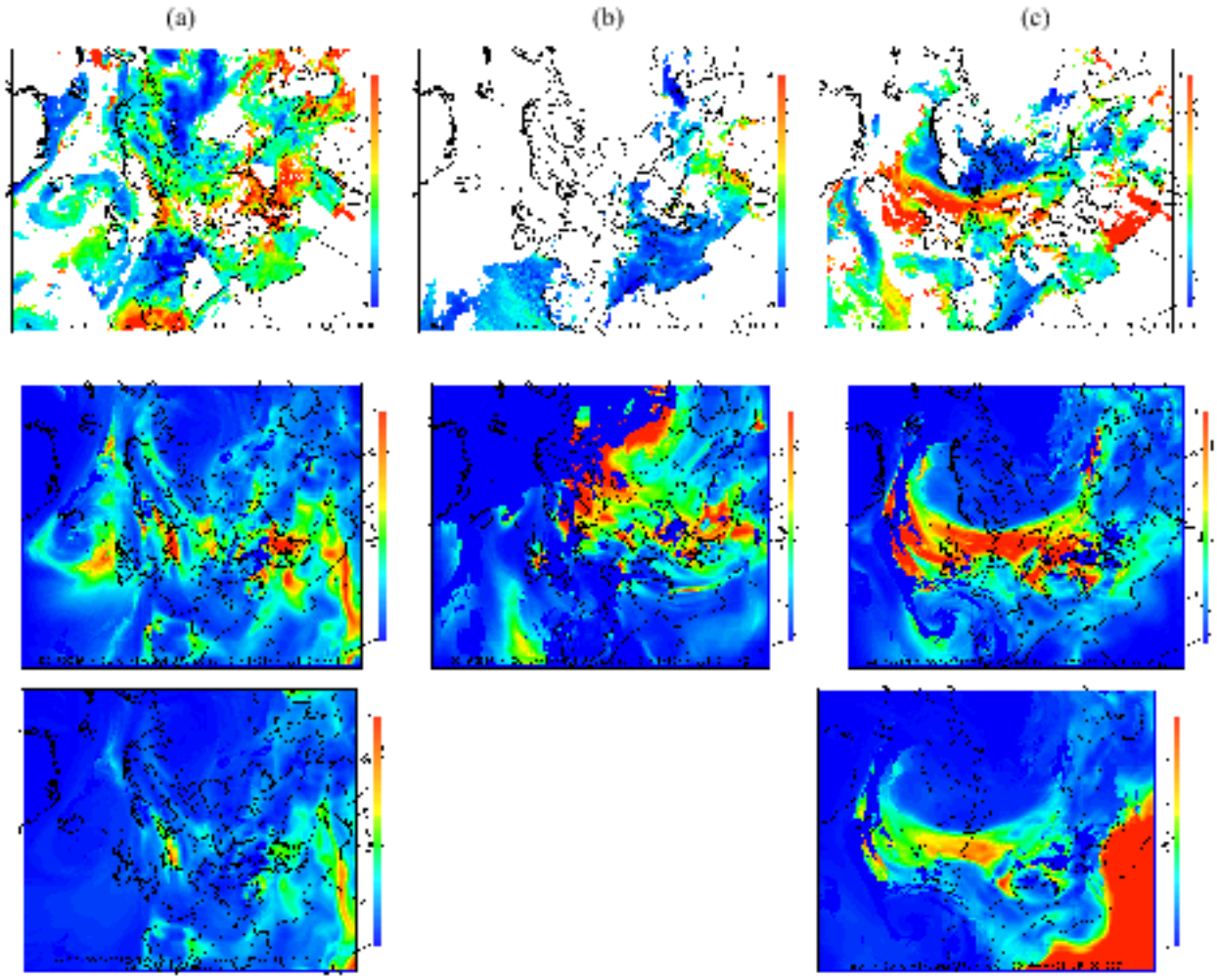

***Figure 6**: Examples of modelled Mie-lognorAOD **(middel panels)** and mass-based AOD **(lower panels)**, compared with MODIS AOD data **(upper panels)** at 0.55 μm wavelength: **(a)** 1 August 2003, **(b)** 1 December 2003, and **(c)** 1 April 2004.*

4.2.1 Comparison of AOD spatial distributions

Table 4 provides a summary of comparison statistics (relative bias and spatial correlation coefficient) between model calculated and MODIS retrieved AOD for the EMEP grid. Here, model and MODIS 0.55 μm AOD are compared at each grid cell for the four 2-month periods. The comparison has been made for the whole EMEP area and for model AOD calculations using the three different approaches: based on aerosol mass concentrations (mass-based), and based on Mie dispersion using a monodisperse aerosol distribution within each size fraction (Mie monodisperse) and a log-normal distribution (Mie log-normal).

The model calculated AOD is lower compared to MODIS retrieved AOD in all cases. The best correspondence with MODIS data is found for AOD calculated using Mie-lognor approach. In this case, the model negative bias is in the range of -51 to -55 % for summer and spring months 2003-2004 and -11% for November-December 2003. The spatial correlation between modelled and MODIS retrieved AOD is rather poor for all seasons, being somewhat better for summer months July and August (0.35 in 2003 and 0.26 in 2004). Using Mie-mono approach gives larger model underestimation of MODIS AOD and lower spatial correlations between calculated and retrieved AOD.

Results from mass-based AOD calculationg lie somewhere between those using Mie scattering with monodisperse and log-normal particle distribution. The model calculated AOD is about 70% lower than MODIS AOD for summer months in 2003 and 2004, and it is 32% lower for November-December 2003.

These results are consistent with verification of model $PM_{2.5}$ surface concentrations with EMEP measurements, which shows that calculated $PM_{2.5}$ is 32% lower than measurements in summer compared to 10% in autumn and 17% in spring for 2004 (Tsyro, 2006 and 2007). The spatial correlation between modelled mass-based AOD and MODIS data varies from 0.30 to 0.45 for different seasons, which is a better result compared to Mie-based AOD calculations.

Table 4: *Relative bias and spatial correlation coefficient of comparison between model calculated Mie-based (monodisperse) AOD, Mie-based (log-normal, and mass-based AOD compared with MODIS retrieved AOD for the EMEP grid.*

		Bias (%)	R		Bias (%)	R
	2003			2004		
Mie-lognor AOD						
	Jul-Aug	-52	0.35	Jul-Aug	-54	0.26
	Nov-Dec	-17	0.11	Mar-Apr	-51	0.11
Mie-mono AOD						
	Jul-Aug	-79	0.31	Jul-Aug	-82	0.17
	Nov-Dec	-58	0.07	Mar-Apr	-77	0.11
Mass-based AOD						
	Jul-Aug	-69	0.49	Jul-Aug	-71	0.36
	Nov-Dec	-32	0.30	Mar-Apr	-62	0.36

Examples of the scatter-plot for modelled versus MODIS AOD (0.55 μm) for the EMEP grid for November-December 2003 and July-August 2004 are given in Fig. 7.

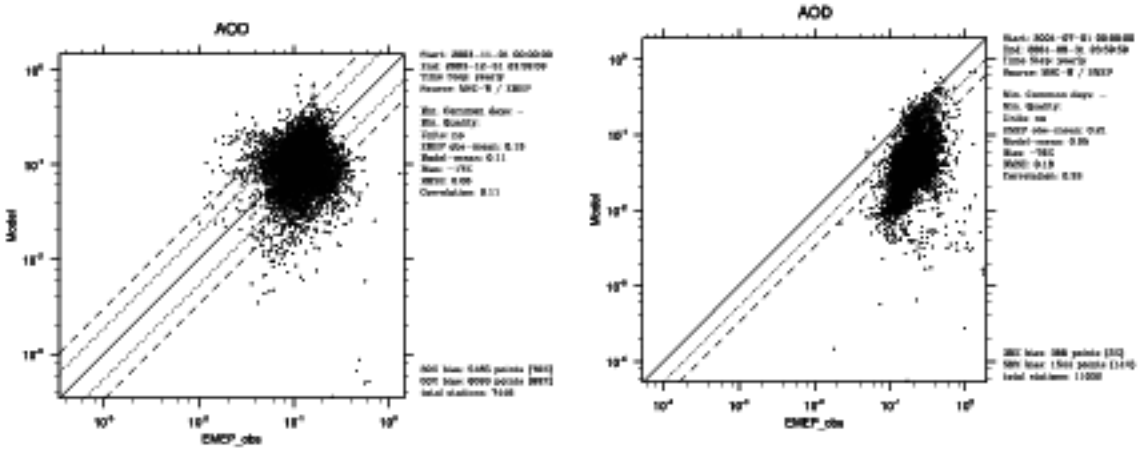

Figure 7: *Scatter-plot for modelled versus MODIS AOD (0.55 μm) for the EMEP grid for November-December 2003 and July-August 2004.*

4.2.2 Comparison of AOD temporal variations

Daily mean model calculated AOD has been compared with MODIS data for a number of grid cells, representing different regions in Europe. Comparison statistics between modelled and MODIS AOD for

several selected areas are summarised in Table 8 (Note that varying number of grid cells were included for different areas).

Table 8: *Comparison of modelled and MODIS AOD for several selected areas (log-normal)*

	July-Aug 2003		Nov-Dec 2003		March-April 2004		July-Aug 2004	
Area	Bias (%)	R	Bias (%)	R	Bias (%)	R	Bias (%)	R
Benelux	-33	0.53	-	-	-18	0.54	-41	0.50
UK	-39	0.65	*23*[*)]	*0.87*	-23	0.45	-47	0.53
Central Europe	-44	0.61	33	0.48	-28	0.30	-54	0.48
SE Europe	-37	0.66	8	0.17	-26	0.37	-29	0.41
central Russia	-59	0.67	*-14*[*)]	*0.29*	-64	0.24	-56	0.18
southern Norway	-65	0.21	-	-	-65	0.37	-71	0.44
Mediterranean Sea	-24	0.05	-18	0.0	-51	0.0	-26	0.23
Southern N. Atlantic	-53	0.28	-33	0.32	-59	0.35	-59	0.0

[*)] *Only 20-25% days with data in the considered period*

The main findings from the comparison are:

- Over land, the model AOD underestimation tends to be larger in summer months, varying mostly between 30 and 70%. This is because of larger model PM underestimation in summer than in other seasons due to not accounted aerosol sources (e.g. secondary organic aerosol, bio-aerosols and emissions from forest fires). On the other hand in cold months, the model AOD results are closer to or even slightly overestimate MODIS AOD (though much less MODIS AOD retrievals are available for autumn-winter season).
- With a few exemptions, the temporal correlation is better for summer months (mostly between 0.4 and 0.65) than in other seasons over land.
- Over remote sea areas (e.g. the southern part of North Atlantic), model underestimates MODIS AOD by 30 to 60%. The temporal correlations for sea areas are rather poor (below 0.3) and are particular low for the Mediterranean Sea.
- For the first time model calculated aerosol properties could be compared with measurements for such regions as in Russia, in south-eastern Europe and Mediterranean Sea (examples in Fig. 8).
- Also here, AOD modelling using Mie scattering approach calculated AOD values for log-normal particle distribution are larger than AOD calculated for monodisperse particles (not shown). Consequently, calculated Mie-lognor AOD is closer to MODIS data than Mie-mono AOD. Also, the correlation between modelled AOD and MODIS AOD appears to be better in the case of log-normal particle distribution.

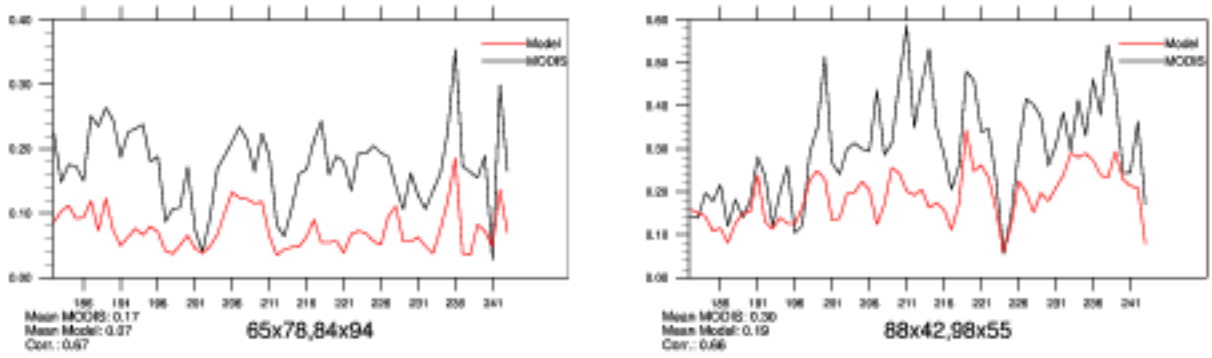

***Figure 8**: Daily time-series of modelled and MODIS AOD for areas in European part of Russia (left panel) and in Southern Europe, i.e. parts of Greece, Albania and Macedonia (right panel) for July-August 2003.*

4.2.3 AOD and surface PM2.5 at EMEP sites

The EMEP model has so far been extensively validated with surface data from EMEP monitoring network. Measurements of PM surface concentrations have been available from EMEP sites since 1999, and comparison results of calculated PM_{10} and $PM_{2.5}$ with observations are presented in EMEP reports (downloadable from http://www/emep/int). Here, we have made a first attempt to look at both calculated and measured surface $PM_{2.5}$ and AOD for the same locations. We have compared AOD calculated with the EMEP aerosol model with MODIS AOD retrievals for the grid cells with the EMEP sites, where surface measurements of $PM_{2.5}$ were available for 2003 and 2004. Main results are outline below.

For summer months (July - August), the model underestimations of MODIS AOD lie between 20 and 55% in 2003 and between 30 and 70% in 2004. The temporal correlation is fairly good (mostly 0.5-0.6) in Central and northern Europe, but it gets worse for some Spanish sites (0.2-0.3). This indicates that a further improvement of windblown dust calculation is needed; including making use of daily Saharan dust fluxes for boundary conditions (monthly Saharan dust concentrations are presently used). Somewhat better correlations are found for 2003 than for 2004.

For spring months (March - April 2004), fewer days with MODIS AOD retrievals than for summer months is available. The model underestimates MODIS AOD by between 25 and 55%. The correlation results are rather mixed for different sites, with the correlation coefficients varying between 0.0 and 0.6.

For late autumn-winter period (November-December 2003), very little AOD retrieval data is available from MODIS for central and northern Europe, as mush data get likely discarded through cloud masking and due to snow/ice surface cover. For some Spanish sites, where MODIS data were available for more than 25% of the days, the model underestimation ranges between 15 and 75%, and the correlation coefficients lie mostly between 0.2 and 0.4.

Figure 9 shows daily time-series of model calculated and MODIS AOD for four EMEP stations.

A joint analysis of $PM_{2.5}$ and AOD results has been made for summer months, for which more MODIS retrieval aerosol data is available. Rather mixed correlations between observed surface $PM_{2.5}$ and MODIS AOD are found for 18 considered stations. In general, the correlation between measured $PM_{2.5}$ and AOD is better for sites in Southern Europe (Spain and Italy), lying mostly between 0.45 and 0.7, while it is lower in Central and Northern Europe (between 0.2 and 0.5) (Fig. 10).

It is interesting to note that for many sites, the correlation between modelled and MODIS AOD is in fact higher than that between calculated and measured $PM_{2.5}$, especially for summer 2003. For instance, the respective correlations are 0.53 and 0.19 for Swiss site Chaumont, 0.51 and 0.22 for Italian site Ispra, 0.55 and 0.17 for Spanish site Visnar (Fig. 10).

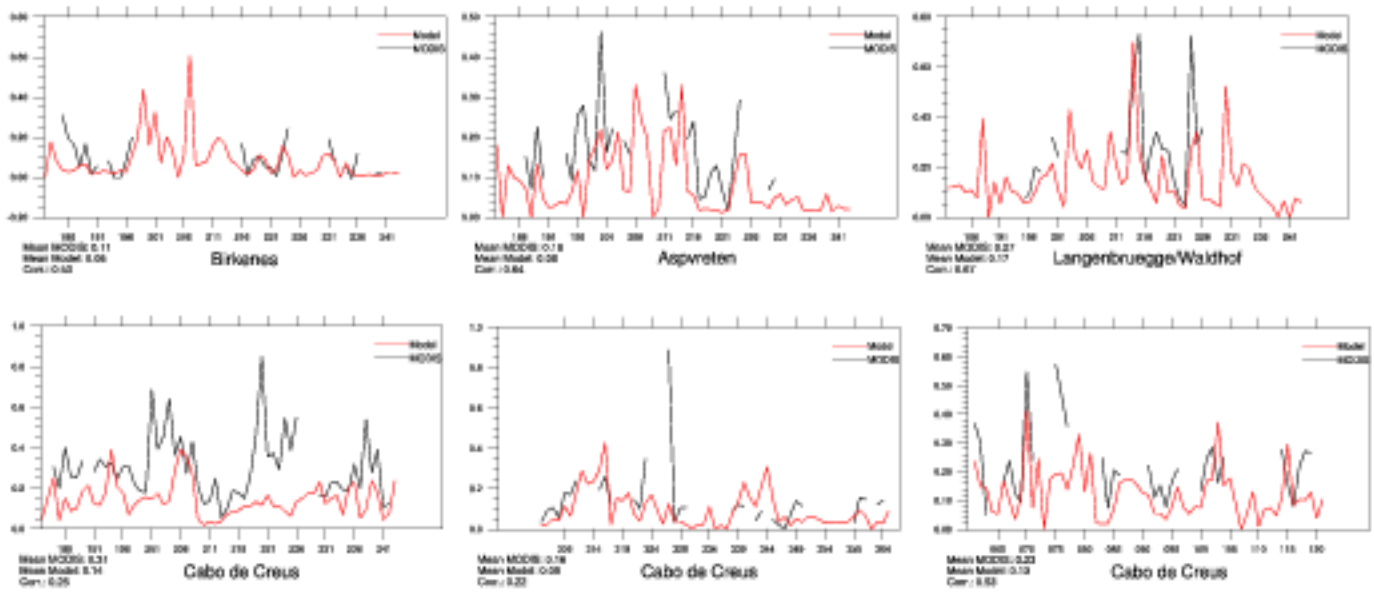

***Figure 9**: Daily time-series of modelled AOD and MODIS AOD for some EMEP stations: upper panel- Birkenes (Norway), Aspvreten (Sweden) and Langenbrügge (Germany) for July-August 2003; lower panel – for Cabo de Creus for July-August and November-December 2003, and March-April 2004.*

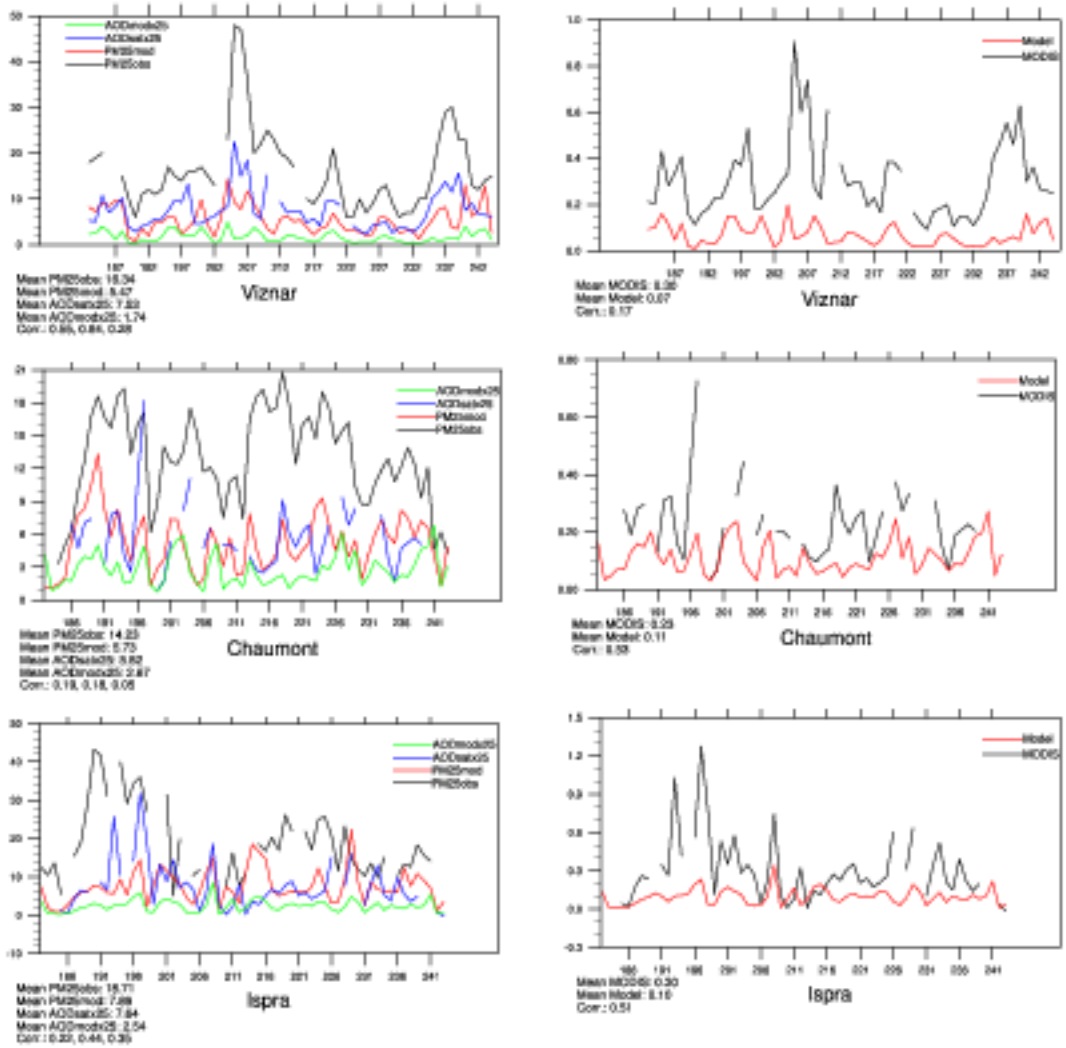

***Figure 10**: Daily time-series for EMEP sites Visnar (Spain), Chaumont (Switzerland) and Ispra (Italy) of: **Left panels** - measured and calculated $PM_{2.5}$ and calculated and MODIS AOD (multiplied by 25 to fit with PM scale); all correlations are with measured $PM_{2.5}$; **Right panels -** calculated and MODIS AOD.*

4.3 Result uncertainties

Comparison of these first simulated AOD results from the EMEP aerosol model with MODIS AOD retrieval data has in general shown a fair agreement in terms of bias and temporal correlations However, the spatial correlation for the whole EMEP grid is not satisfactory. Also, considerable discrepancies between modelled and MODIS AOD are found for some periods and regions. While analysing the results, it is important to keep in mind that there are non-negligible uncertainties in both the model AOD results and MODIS AOD retrievals.

4.3.1 Uncertainties in MODIS AOD data.

Among the main uncertainties in MODIS AOD retrievals are those due to:

- over ocean – some clouds and sun glint data contamination; dust with non-spherical geometry;
- over land – uncertainties in surface reflection; sub-pixel snow, ice or surface water; cloud data contamination.

Dependant on how many contaminated pixels were discarded, each of 50x50 km^2 EMEP grid cell may aggregate a different amount of AOD data. This means that grid cells will have varying data coverage and that the representativeness of MODIS AOD data will vary from grid cell to grid cell.

Besides, MODIS AOD retrieval algorithms rely upon prescribed aerosol types ("aerosol models"), which are assigned pre-computed optical properties, based on AERONET data. An "aerosol model" consists of one fine and one coarse aerosol mode, which are chosen from among four fine and five coarse pre-described aerosol modes in the over-ocean retrieval algorithm. In the over-land retrieval uses a priori assigned fine aerosol types for four seasons, aggregated on 1° x 1° grid globally. For instances, the non-absorbing "aerosol model", representing urban/industrial pollution, is chosen for Western Europe, whereas neutral aerosol type (generic/forest fires aerosol) is assumed the rest of the EMEP grid. This means that the ambient aerosol profiles and composition as assumed in MODIS retrievals and calculated with the EMEP model will differ.

Moreover, MODIS retrieval algorithm does not seem to take into account the dependence of aerosol optical properties on ambient relative humidity. Furthermore, the complex refractive indices are not necessarily the same in the model and MODIS retrievals (e.g. we have assumed somewhat smaller scattering for soluble particles and larger absorptions for black carbon than used in MODIS retrievals). Thus, the optical properties of aerosols will differ in the model and MODIS calculations. This is another likely cause of discrepancies in modelled and MODIS AOD.

4.3.2 Uncertainties in modelled AOD.

The correctness of model AOD results depends, on one hand, on the model's ability to accurately calculate aerosol atmospheric concentrations and size distribution and, on the other hand, on the accuracy with respect to modelling aerosol optical properties. The latter relies on the choice of complex refractive indices for different aerosol components and on how the effective refractive indices are derived, and it depends on the representation of aerosol size distribution.

AOD modelling using Mie-dispersion algorithm for size-resolved aerosols is based on model calculated particle number concentrations and size distribution, which in turn, are associated with considerable uncertainties. This is mainly because of the lack of data on the size distribution of particle emission and missing aerosol sources, but also due to uncertainties in modelling aerosol dynamic processes, i.e. nucleation, coagulation and condensation. On the other hand, using complex refractive indices to calculate extinction efficiencies and cross-sections for size-resolved particles represent a sounder parameterisation than the mass-based one. Still, there are uncertainties in complex refractive index values for different aerosol components, uncertainties related to aerosol mixing state and thus derivation of the effective refractive index. Furthermore, particle deviation from a spherical form assumed for Mie-scattering calculations gives rise to inaccuracy in AOD modelling, especially for dust dominated aerosol loading.

A mass-based AOD scheme makes use of model calculated mass concentrations of different aerosol components. As shown in annual EMEP reports (e.g. Tsyro, 2004 and Tsyro, 2006), model performance for aerosol mass is presently better than its performance for particle number concentrations and size distribution compared to observations. However, our results indicate that AOD modelling based on the aerosol total mass is less accurate than AOD calculations based on size resolved aerosol extinction efficiencies (AOD Mie-lognor) in terms of reproducing MODIS AOD maps (Fig.6). In particular, the effect of light extinction by Saharan dust is exaggerated in mass-based AOD calculations.

4.3.3 Sensitivity tests of AOD results to primary emitted particle sizes.

As it was described in Section 3.1, there is presently no appropriate information about the size distribution of primary particles emitted from anthropogenic sources. In the EMEP model, rather crude assumptions on the size of primary particles were made in order to derive the number of particles emitted in the Aitken and the accumulation fractions from primary $PM_{2.5}$ emissions.

Preliminary sensitivity tests have shown that decreasing the diameters of primary emitted Aitken particles from 0.04 μm to 0.03 μm and accumulation particles from 0.4 μm to 0.3 μm leads to increases of the annual mean particle number concentrations by 75-120% in the Aitken fraction and by 35-75% in the accumulation fraction (Fig.11, left). At the same time, annual mean diameters of Aitken and accumulation particles have decreased respectively by 5-15% and by 10-17% (Fig.11, middle) (diameters of Aitken particles increased by 5-10% over ocean). The combined effect of increased particle number and decreased particles size is a general decrease of AOD by 5 to 20% over land and by 1-5% over the ocean. Thus, in this case, the effect of decreased aerosol scattering cross-sections overrides the effect of increased particle number.

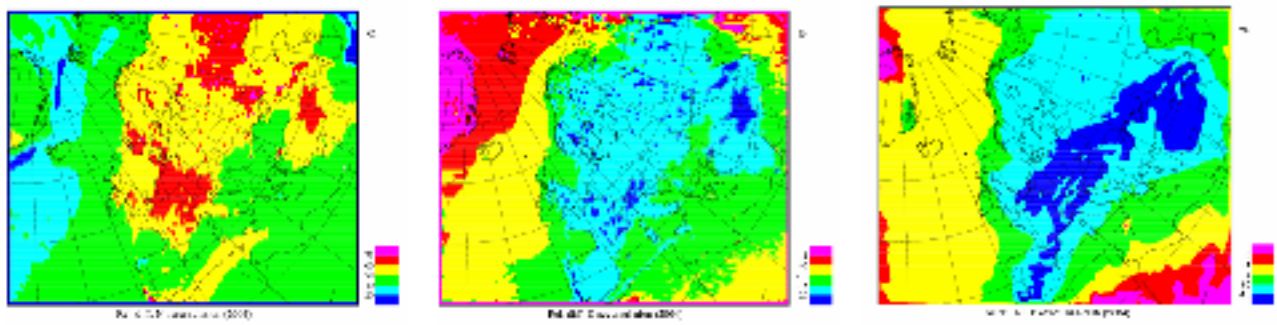

***Figure 11**: Relative changes in the annual mean number (left) and diameter (middle) of accumulation particles, and AOD, as the diameter of primary emitted Aitken particles decrease from 0.04 μm to 0.03 μm and the diameter primary emitted accumulation particles is decreased from 0.4 μm to 0.3 μm. Year: 2004*

5 Summary and outlook

An "observation operator" to the EMEP aerosol model has been developed for simulations of Aerosol Optical Depth (AOD), which can be either operating online within the model or independently using aerosol concentration results from the transport model. In the present work, the observational operator has been implemented in the EMEP aerosol model. Two AOD calculation schemes have been tested within the model: a simplified one, based on aerosol mass concentrations, and the one based on the Mie scattering mathematical formalism for size-resolved particle number concentrations. The particles are assumed to be spherical and internally mixed. In this work, we have calculated AOD at a wavelength of 0.55 μm, for which MODIS "Joint ocean-and-land" AOD product is available.

To achieve CPU efficient AOD simulations, the model employs a priori prepared a look-up table for particle extinction efficiency. Two lookup tables have been made using a Mie scattering program developed by Mishchenko (2005): one for monodisperse particles and one for log-normally distributed

particles within each of four size fractions in the aerosol model. The resulting extinction efficiencies for log-normal aerosol distribution are somewhat larger than those for monodisperse aerosols.

In this report, we present calculation results of AOD at 0.55 μm for the years 2003 and 2004, using three different approaches: one scheme based on aerosol mass concentrations, and two schemes based on size-resolved aerosol numbers and using Mie scattering lookup table for monodisperse aerosols and for log-normally distributed aerosols.

Model calculated AOD has been compared with MODIS AOD retrievals for four 2-month periods in 2003 and 2004, representing different seasons. On average, model calculated AOD is lower compared to MODIS data for all seasons. The best correspondence with MODIS data is found for AOD calculated using Mie-log-normal approach. In this case, the model negative bias is in the range of -51 to -55 % for summer and spring months and -11% for late autumn-winter months. The spatial correlation between modelled and MODIS retrieved AOD is rather poor for all seasons, being somewhat better for summer months July and August (0.35 in 2003 and 0.26 in 2004).

Model calculated daily AOD has been compared with MODIS data for a number of grid cells representing different regions in Europe and also for the grid cells with EMEP monitoring stations. Over land areas, the model AOD underestimation tends to be larger for summer months (30-70%), which is probably due to not accounting for secondary organic aerosol, bio-aerosols and emissions from forest fires. For cold months, the model appears to slightly overestimate MODIS AOD over land, though much less MODIS AOD retrievals are available for these months. With a few exemptions, the temporal correlation is better for summer months (mostly between 0.4 and 0.65) than in other seasons over land. Over remote sea areas (e.g. the southern part of North Atlantic), model underestimates MODIS AOD by 30-60%. The temporal correlations for sea areas are rather poor (below 0.3) and are particular low for the Mediterranean Sea.

Using the assumption of monodisperse aerosols in the size fractions, gives a larger model underestimation of MODIS AOD and lower spatial correlations between calculated and retrieved AOD compared to the results using log-normal particle distribution. The results from mass-based AOD calculations are somewhere between those using Mie scattering with monodisperse and log-normal particle distribution. It should be pointed out that employing the satellite data has allowed for the first time evaluating modelled aerosols with measurements for a number of regions where no surface aerosol observations are available (e.g. Russia, south-eastern Europe and Mediterranean Sea).

For the EMEP sites with measurements of surface PM concentrations, we have made a joint analysis of the results for both calculated and measured surface AOD and $PM_{2.5}$. Rather mixed correlations between observed surface $PM_{2.5}$ and MODIS AOD are found for different stations. In general, the correlation between measured $PM_{2.5}$ and AOD is better for southern European sites, lying mostly between 0.45 and 0.7, while it is lower for central and northern Europe (between 0.2 and 0.5). The interesting result is that for many sites, the correlation between modelled and MODIS AOD is higher than the correlation between calculated and measured $PM_{2.5}$, especially for summer 2003.

Summarising, first model calculations of AOD at 0.55 μm and comparison of the model results with MODIS AOD retrievals has shown fairly promising results. However, it is recognised that the uncertainties in both model results and MODIS data may affect the comparison results. The main uncertainties in modelled AOD are those associated with the size distribution of primarily emitted particles, with aerosol dynamics parameterisations, with the aerosol mixing state in refractive index computations, and the effect of non-spherical particles. In future, it is envisaged to perform a series of sensitivity test to study the effects of different uncertainties on model AOD result.

References

Bond T. C., and R. W. Bergstrom (2006) "Light Absorption by Carbonaceous Particles: An Investigative Review", *Aerosol Science and Technology*, 40:1, 27-67.

Hale, G.M., and M.R. Querry (1973). Optical constans of water in the 200-nm to 200-mm wavelength region. *Appl. Opt*., 12, 555-563.Holben, B. N., T. F. Eck, et al. (1998). "AERONET – A federated instrument network and data archive for aerosol characterization. "Remote Sensing of Environment 66(1):1-16.

Gomes, L., Rajot, S.C., Alfaro, S.G. and A. Gaudichet. (2003). Validation of a dust production model from measurements performed in semi-arid agricultural areas of Spain and Niger. - *Catena*, 52, p. 257-271.

Kinne, S et al. (2006). An AeroCom initial assessment – optical properties in aerosol component modules of global models. *Atmos. Chem. Phys*. 6, 1815-1834.

Kirkevåg, A., T. Iversen, Ø. Seland, J. E. Kristjánsson (2005). "Revised schemes for aerosol optical parameters and cloud condensation nuclei in CCM-Oslo, *Institute Report series, 128*, Department of Geosciences, University of Oslo, ISBN 82-91885-31-1, ISSN 15016854-128.

Kupiainen, K. and Z. Klimont (2006). Primary emissions of fine carbonaceous particles in Europe. - *Atmos. Environ*., doi:10.1016/j.atmosenv.2006.10.066.

Köpke, P., Hess, M., Schult, I., and E.P. Shettle (1997). Global Aerosol Dataset. Report No. 243. Max-Plank-Institut für Meteorologie. Bundesstrasse 55, D-20146, Hamburg, Germany.

Mishchenko. M. I., 2005: The program computes far-field light scattering using the Lorenz-Mie theory, and is developed by M. I. Mishchenko at NASA Goddard Institute for Space Studies, New York. The program is based on the book "Scattering, Absorption, and Emission of Light by Small Particles" by M. I. Mishchenko, L. D. Travis, and A. A. Lacis (2002). Cambridge University Press, Cambridge, England. https://www.giss.nasa.gov/~crmim.

Marticorena, B. and G. Bergametti (1995). Modelling the atmospheric dust cycle: 1. Design of a soil driven dust emission scheme. - *J. Geophys. Res*., 100, D8, 16415-16430.

Pirjola, L., Tsyro, S., Tarrason, L., and M. Kulmala (2003). A monodisprse aerosol dynamics module, apromising candidate for use in long-range transport models: Box model tests. *J. Geophys. Res*., 108, D9, 4258, doi:10.1029/2002JD002867.

Remer, L.A., D. Tanré, and Y.J. Kaufman (2006). Algorithm for remote sensing of tropospheric aerosol from MODIS: Collection 5. Product ID: MOD04/MYD04). NASA Goddard Space Flight Center, Code 913, Greenbelt, MD 20771, USA. http://modis.gsfc.nasa.gov/data/atbd/atbd_mod02.pdf

Seinfeld, J. H., S. N. Pandis (1997), "Atmospheric Chemistry and Physics; From Air Pollution to Climate Change". Wiley-Interscience, New York, USA.

Simpson, D., Fagerli, H., Jonson, J. E., Tsyro, S., Wind, P., and Tuovinen, J.-P.: Transboundary Acidification, Eutrophication and Ground Level Ozone in Europe. Part I. Unified EMEP Model Description. EMEP/MSC-W Status report 1/2003 Part I. Norwegian Meteorological Institute, Oslo, Norway, 2003. http://www.emep.int.

Sokolik, I.N., and O.B Toon (1999). Incorporation of mineralogical composition into models of the radiative properties of mineral aerosol from UV to IR wavelengths. *J. Geophys. Res*., 104, D8, 9423-9444.

Tsyro, S. (2006). Model assessment of particulate matter in Europe in 2004. In: Yttri, K. E. and Torseth, K. (eds.) Transboundary Particulate Matter in Europe, EMEP Status Report 4/2005. Norwegian Institute for Air Reseach, Kjeller, Norway.

Tsyro, S. (2004). Model assessment of particulate matter in Europe in 2002. In: Torseth, K. (ed.) Transboundary Particulate Matter in Europe, EMEP Status Report 4/2004. Norwegian Institute for Air Reseach, Kjeller, Norway.

Tsyro, S. (2002) First estimates of the effect of aerosol dynamics in the calculation of PM10 and PM2.5. MSC-W Note 4/02. Norwegian Meteorological Institute, Oslo, Norway.

Tegen, I., Hillrig, P., Chin, M., Fung, I., Jacob, D., and J. Penner (1997). Contribution of different aerosol species to the global aerosol extinction thickness: Estimates from model results. *J. Geophys. Res*, 102, D20, 23,895-23,915.

WHO (2006). Health risk of particulate matter from long-range transboundary air pollution- Joint WHO/UNECE Convention Task Force on the Health Aspects of Air Pollution. World Health Organisation, European Centre for Environment and Health, Bonn Office.